

10

20



# Late Holocene cooling and increased zonal asymmetry in the midlatitude North Atlantic

Weimin Si<sup>1</sup>, Timothy Herbert<sup>1</sup>, and John Robbie Toggweiler<sup>2</sup>

- 5 <sup>1</sup> Brown University, Earth, Environmental and Planetary Sciences, Providence, RI, United States
  - <sup>2</sup> Geophysical Fluid Dynamics Laboratory, National Oceanic and Atmospheric Administration, Princeton, NJ, 08540-6649, USA

Correspondence to: Weimin Si (weimin si@brown.edu)

Abstract. Sea Surface Temperature reconstructions derived from alkenone biomarker (SST-alk) reveal a cooling trend in the North Atlantic during the late Holocene (the last 5,000 years), contrary to the warming simulated by transient climate models driven by 20 ppm increase in greenhouse gas concentrations. It has been suggested that the apparent cooling in paleo-records may reflect the evolution of summer temperatures, a seasonal signal biased by the preferential growth of haptophyte algae during warm months. Here, we investigate the spatial pattern of SST-alk changes and show that late Holocene cooling is characterized by an increased zonal SST gradient in the mid-latitude North Atlantic, with greater cooling in the west than in the east. Multiple proxies indicate that this increase in zonal asymmetry is associated with reorganizations of the inter-gyre ocean circulation. We find that transient simulations, such as TraCE-21k, do not reproduce the zonally asymmetric cooling and the inferred changes in inter-gyre circulation from the mid- to late Holocene. This misrepresentation of spatial and temporal variability likely explains the data-model discrepancy in the mid-latitude North Atlantic.

#### 1 Introduction

Estimates of global temperature changes over the Holocene (from  $\sim$ 11.6 ka to the present) reveal large discrepancies between proxy reconstructions and climate model simulations. Climate models typically produce gradual global warming in response to a 20 ppm increase in pCO<sub>2</sub> in the last  $\sim$ 5 kyrs (Erb et al., 2022; Liu et al., 2014; Osman et al., 2021). In contrast, a variety of paleoclimate archives from both terrestrial and marine realms indicate an overall cooling trend in the Northern Hemisphere following the mid-Holocene thermal optimum ( $\sim$ 6-10 kyrs ago) (Kaufman et al., 2020; Linsley et al., 2010; Marchal et al., 2002; Marcott et al., 2013; Shuman and Marsicek, 2016). This discrepancy between model simulations and proxy data is known as the "Holocene conundrum" (Liu et al., 2014).

One often-invoked explanation for model-data inconsistency is biases in proxy reconstructions (Bova et al., 2021; Leduc et al., 2010; Liu et al., 2014). Summer-growing species, for example, may primarily record changes in summer conditions rather than long-term shifts in annual means. As a result, the cooling observed in the Northern Hemisphere during the late



35

50

60



Holocene has been attributed to summer cooling, driven directly by declining summer insolation. On the other hand, biases can also arise in model simulations (He & Clark, 2022; Liu et al., 2018; Park et al., 2019; Thompson et al., 2022), leading to systematic model—data discrepancies that potentially obscure our understanding of climate sensitivity to different forcings, particularly CO<sub>2</sub> versus orbital forcing. A recent study, for instance, suggests that precession can directly drive warming and cooling at lower latitudes and may therefore play a role in global Holocene cooling (Toggweiler and Si, 2025).

A useful approach to gain insights into the origin of the model-data discrepancy is to investigate the spatial characteristics of regional climate and their temporal evolution. Such analyses may help diagnose the dynamics driving both local and global climatic variations. The North Atlantic is of particular interest in this context because it exhibits a notable data-model gap, with proxy compilation indicating pronounced cooling (Marcott et al., 2013) whereas climate models predicting a warming trend (Liu et al., 2014; Osman et al., 2021). Based on SST proxies in the Norwegian Sea and the eastern North Atlantic, previous studies have suggested that the cooling might be linked to local and/or remote (e.g. North Pacific) changes in ocean-atmosphere circulation (Andersson et al., 2010; Kim et al., 2004).

In this study, we integrate alkenone SST (SST-alk), productivity and planktonic foraminiferal assemblages with previous published data to investigate mid- to late Holocene SST changes in relation to ocean circulation changes in the mid-latitude North Atlantic (35-65°N, 80-0°W; Figure 1a). We then conduct a model–data comparison to demonstrate that the spatiotemporal patterns inferred from proxy records are not adequately captured by model simulations.

#### 2 Wind-driven inter-gyre circulation in the North Atlantic

To facilitate the discussion, we first characterize oceanography in the mid-latitude North Atlantic, following the concept of inter-gyre circulation (Marshall et al., 2001). The inter-gyre region refers to the wind-driven circulation that straddles the mid-latitude North Atlantic (Czaja and Marshall, 2001; Marshall et al., 2001). Today, positive wind stress curl north of this region drives a cyclonic subpolar gyre, while negative wind stress curl to the south drives an anticyclonic subtropical gyre. The zero wind stress curl line thus marks the confluence of the two gyres. Heat and fluid properties are transported from both the subtropical and subpolar gyres into this frontal zone, and their respective contributions are thought to be critical for salt and heat transport into the Nordic Seas.

In the current climatic state, the climatological mean of the zero wind-stress-curl line has a characteristic SE-NE tilt across the mid-latitude North Atlantic, coincident with the location where the Gulf Stream detaches from the slope and feeds into the North Atlantic Current (NAC) (Marshall et al., 2001). In the SST field (Figure 1a), this is expressed as a band of 10°C water extending diagonally from Cape Hatteras to the south of Iceland (shown as the dark-green band in the SST field). This 10 °C water also marks the core of the NAC (Rossby, 1996), which acts as the boundary flow separating the subtropical and



70

90



subpolar gyres in the mid-latitude North Atlantic. As the extension of the Gulf Stream, the NAC carries warm and saline subtropical water into subpolar latitudes. The spatial configuration of this inter-gyre circulation plays a key role in maintaining the zonal SST and salinity gradients in the mid-latitude North Atlantic, with relatively cold and fresh subpolar water to its NW and warm, saline subtropical waters to its SE.

On decadal timescales, changes in the position and orientation of the zero wind-stress-curl line are tightly linked to anomalous inter-gyre circulation (Marshall et al., 2001; McCarthy et al., 2015; Volkov et al., 2019; Yang et al., 2020). When the zero-curl line is more zonal and equatorward, the boundary flow becomes more W-E oriented and transports less heat meridionally (Häkkinen et al., 2011; Newell & Hsiung, 1987), and vice versa. Indeed, the tilted orientation of the coupled wind and gyre circulations in the mid-latitude North Atlantic is critically linked to the deepwater formation in the North Atlantic (Emile-Geay et al., 2003; Warren, 1983).

The sites examined in this study are mostly aligned with the 10°C isotherm in the mid-latitude North Atlantic (Figure 1a). We use these sites to monitor changes in inter-gyre circulation over time. In section 6, we present evidence of a dynamically shifting inter-gyre frontal system during the Holocene. In section 7, we show that transient simulations did not capture either the mean geometry of the inter-gyre circulation or its variability during the Holocene.

#### 3 Seasonality of SST-alk in the North Atlantic

We also want to evaluate the seasonality of the SST-alk data before using them in paleoceanographic interpretations. Primary productivity in the open ocean is largely controlled by a combination of light availability and nutrient supply to the mixed layer. The seasonal variations in these limiting factors largely determine the timing of phytoplankton blooms. In the North Atlantic, this process is manifested as the meridional propagation of "spring" blooms from mid-latitudes in February/March to higher latitudes in August/September (Siegel et al., 2002). An often-invoked explanation for the Holocene conundrum, therefore, suggests that biogenic paleo-proxies may record the temperatures during the organisms' growing seasons rather than annual mean temperatures. The late-Holocene cooling is then attributed to changes in seasonality driven by reduced local summer insolation (Bova et al., 2021; Leduc et al., 2010).

Here, we calculate productivity-weighted SST by computing the monthly mean (Huang et al., 2021), weighted by monthly primary productivity derived from satellite-based chlorophyll measurements (Losa et al., 2017). We then compute the differences between this productivity-weighted SST and the annual-mean SST. Two features stand out in the difference map (Figure S1). First, for most of the low-latitude ocean, the productivity-weighted SST "coincides" with the annual mean temperature, resulting in small seasonal biases (indicated by green colors in Figure S1). In contrast, the productivity-weighted SST exhibits large positive anomalies relative to the annual mean in the mid- and high-latitude regions of the North



105

110

115

130



Atlantic and North Pacific (shown in warm colors in Figure S1), suggesting a bias linked to the seasonal growth of phytoplankton.

Next, we estimate core-top SST-alk using the calibration of Müller et al., (1998) and calculate their deviations from the modern annual mean (circles in Figure S1). A similar calculation was employed by Tierney and Tingley (2018). The results show that productivity-weighted SST and coretop SST-alk share similar spatial pattens in their deviations from the annual mean SST. This spatial coherence between expected and observed biases thus supports the idea that SST-alk reflects the surface temperature during the principal growth season(s) of alkenone producers, particularly in the mid-latitudes. Regressing mid- and high-latitude North Atlantic and North Pacific SST-alk values against productivity-weighted SST, rather than annual mean, reduces the Root Mean Square Deviation by about 25% (Figure S2).

#### 4 Materials and Methods

Two IODP cores are analyzed in this study for alkenone SST (ODP U1304 and ODP U1308, Figure 1). Age models of two cores are constrained by <sup>14</sup>C dates and the AZ1 tephra layer associated with the Younger Dryas. The latter has been dated to 12.1 ka (Hodell et al., 2010; Thornalley et al., 2011). For <sup>14</sup>C analysis, ~20 mg of a single species, *G. bulloides*, from the >125 μm fraction, were picked from each sample and ultrasonically cleaned in 3% H<sub>2</sub>O<sub>2</sub> and DI water before being leached 10% with dilute HCl to remove potential diagenetic overgrowth and contamination. Radiocarbon analyses were conducted at Keck Carbon Cycle AMS lab at the University of California Irvine. Calendar ages were subsequently calculated using the Matlab package *Undatable* (Lougheed and Obrochta, 2019) based on Marine13 calibration curve. All age data control points are included in Supporting Table 2.

For alkenone analysis, ~2 grams of dry sediments were freeze-dried and extracted using an automated pressurized fluid extraction device (ASE 200). Extractions were carried out at 150°C and 1500 psi and consisted of three static cycles. For each cycle, ~10 ml 100% methylene chloride was flushed through the sample cell. Total lipids extracts were then dried under a nitrogen stream and redissolved in 100% hexane. In order to obtain a clean alkenone profile and avoid potential co-elution, silica gel columns were used to isolate the alkenone fraction. A silica gel column of ~4 cm was rinsed with hexane before loading organic extracts. The organic extract was then transferred onto the column and eluted with ~4 ml hexane, followed by 4 mL methylene chloride. Alkenones were recovered in the methylene chloride fraction.

Alkenone concentration was quantified on a Gas Chromatography (Agilent 6890) equipped with a flame-ionization detector. Alkenone fractions recovered from the silica gel columns were reconstituted using 200 µl of toluene, which was previously spiked with n-hexacontracontane (C36) and n-heptatriacontane (C37) standards of known concentrations. The chromatographic column used was a DB-1 (60-m length, 0.32-mm diameter, and 0.10-µm film thickness). The GC

https://doi.org/10.5194/egusphere-2025-5181 Preprint. Discussion started: 29 October 2025

© Author(s) 2025. CC BY 4.0 License.



135

140

145

150

160

EGUsphere Preprint repository

temperature program started at an initial temperature of 90 °C and held for 2 min before ramping at an initial rate of 40 °C/min to 255 °C, then ramping slowly at a rate of 1 °C/min to 300 °C. The final ramp was at a rate of 10 °C/min to 320 °C, with an 11 min hold time. To better take into account analytical uncertainties, a random number of samples from each core are re-analyzed on the same GC-FID using RTX-200 column. The RTX-200 column has a different polarity relative to DB-1 and thus can help detect possible coelution.

For planktonic foraminiferal analysis, dry samples from ODP U1304 were washed through a 20 μm sieve and oven-dried at ~60°C. Foraminifera >125 μm were then divided into small splits using a Riffle Splitter. From each subsample, all foraminiferal specimens were picked and archived on microfossil slides, with approximately 300 specimens picked per sample. Our faunal analysis focuses on the relative abundance of four end-member groups, tropical-subtropical (*Globigerinoides ruber - Globigerinoides sacculifer*), Gulf Stream transitional (*Globorotalia inflata*), subpolar (*Globigerina bulloides*) and polar (*Neogloboquadrina pachyderma*) species (Figure 2 legend). The validity of this faunal analysis, compared to the traditional CLIMAP faunal assemblage approach, which documents the entire foraminiferal fauna, has been demonstrated both empirically and statistically (Jonkers and Kučera, 2019; Ruddiman and Esmay, 1987).

Spatial ΔSST-alk over the late Holocene is calculated from the mean estimates of two time slices (6-8 ka) and (0-2 ka) using a combination of existing alkenone (Supporting Table 1 for a complete reference list) and new analyses from the North Atlantic (Figure 1a). For previously published records, age models are taken directly from the original publications without modification. In cases where downcore SST-alk data are unavailable for the last 2 kyr, core-top alkenone data from nearby locations are used instead (Supporting Table 3).

# 5 Results

The spatial pattern of ΔSST-alk between the two time slices 6-8 ka and 0-2 ka is shown in Figure 1b, with blue numbers indicating the magnitude of cooling. Overall, we find that the greatest cooling occurred in the western basin, with a maximum value of ~4.9°C at GGC30. In contrast, cooling is muted in the eastern basin, where subtropical water dominates.

In the downcore time series, SST-alk from ODP U1304 (Figure 2d Red line) exhibits warm durations of the Bølling–Allerød (13-14 ka) and the mid-Holocene (~6-11.6 ka), followed by cold conditions during the Younger Dryas (~11.6-12.9 ka) and the late Holocene (0-6 ka), respectively. SST-alk over the last 2 kyrs averages ~10.3°C, which is ~1.5°C warmer than the modern annual mean (~8.8°C). As discussed above, this warm bias likely reflects the preferential summer production of alkenones at 50°N.





Total alkenone concentration (C37<sub>total</sub>), which is considered a proxy of primary productivity (Lawrence et al., 2006; Raja and Rosell-Melé, 2021), was low during Heinrich Event 1 and the Younger Dryas (Figure 2c). During the Holocene, C37<sub>total</sub> shows a gradual increase between ~11.6-8.2 ka, followed by a decline after ~6 ka.

Planktonic foraminiferal analysis of ODP U1304 also reveals changes throughout the Holocene. Between 8-10 ka, tropical and subtropical surface species such as *G. ruber* and *G. sacculifer* were present at this 50°N site (Pink shading in Figure 2d).

170 Meanwhile, *G. inflata*, typically indicative of the Gulf Stream thermocline, became particularly abundant. Beginning ~8 ka, however, the subpolar species *G. bulloides* became dominant. On the other hand, the polar species *N. pachyderma* accounted for a large portion of the assemblage during the Younger Dryas and the earliest Holocene. Its relative abundance, however, has remained low since ~8.2ka.

#### 175 6 Discussions

180

# 6.1 Increased zonal SST gradient in the late Holocene

The spatial distribution of ΔSST-alk in Figure 1b suggests that the cooling in the mid-latitude North Atlantic over the last 6 kyrs was zonally asymmetric, with a larger temperature decrease west of the inter-gyre region than to the east. Considering the seasonality of the alkenone proxy (section 3), the cooling is best described as an increase in the summertime zonal SST gradient in the mid-latitude North Atlantic. The implication is that the cooling must have arisen from processes that also help maintain the zonal asymmetry in modern SST, rather than being a simple *direct* response to local insolation changes (Leduc et al., 2010), which would have produced a zonally uniform cooling.

What could have contributed to the increased zonal SST gradient? As briefly reviewed in Section 2, the zonal asymmetry in the mid-latitude North Atlantic is primarily associated with the inter-gyre frontal system. The position, orientation, and strength of the inter-gyre circulation can significantly influence air—sea heat fluxes, Ekman transport, and eddy activity (Häkkinen et al., 2013; Marshall et al., 2001; Marzocchi et al., 2015; Newell & Hsiung, 1987), and therefore shape regional SST distributions.

Based on the spatial pattern of ΔSST-alk in Figure 1b, we thus speculate that: (1) During the early and mid-Holocene, the time-averaged summertime inter-gyre circulation was positioned farther north and oriented in a southwest–northeast (SW–NE) direction (Figure 3a). As a result, sites near the modern 10°C isotherm were more strongly influenced by subtropical waters and recorded warmer SSTs. The SW-NE tilt also directed the NAC into the Nordic Sea, promoting warming at high latitudes; (2) In the late Holocene, the inter-gyre circulation likely shifted equatorward, causing pronounced cooling at sites proximal to the present-day 10°C water.



200

205

210

215

220



# 6.2 Evidence of Changes in inter-gyre circulation

# 6.2.1 Inter-gyre circulation during the warm early and mid-Holocene

To test our hypothesis (Figure 3a), we first examine foraminiferal assemblages, whose distribution is strongly influenced by the Gulf Stream and the NAC (Ruddiman, 1968). During the earliest Holocene (~11-12 ka), we see a rapid decrease in the relative abundance of the polar species *N. pachyderma* in ODP U1304 as SST-alk increased (Figure 2d, Blue shading and red line). During the early Holocene warm period (11-8 ka), the arrival of warm water species, including tropical *G. ruber* and "Gulf-stream" subsurface species *G. inflata* (Figure 2d, Pink and Yellow shading), suggests either a more northerly position of the Gulf Stream or enhanced northward heat transport. This would have led to warmer, more subtropical-like surface conditions at ODP U1304 (53°N). It is also consistent with the Mg/Ca SST estimate from ODP 984 (61°N, Came et al., 2007) and fossil records from higher latitudes. The presence of thermophilus mollusks from Svalbard (Salvigsen et al., 1992), for instance, suggests that warm Atlantic waters had already reached the Fram Strait by 9.5 ka. Diatom records also suggest that Atlantic assemblages became more prevalent in the southern Nordic Sea by 9.5 ka and dominated the region between 8.8 and 7 ka (Koç et al., 1993).

Additionally, low IRD content on the East Greenland shelf and low Quartz content (expressed as the ratio of Qrtz/Plag) just north of Iceland are interpreted as evidence of an enhanced influence of the Atlantic-sourced warm Irminger Current and stronger ocean heat transport during the mid-Holocene (Figure 2a), This likely led to the retreat of Greenland's tidewater glaciers and reduced sea ice influx from the Greenland Sea (Moros et al., 2006; Perner et al., 2016; Werner et al., 2013).

#### 6.2.2 subpolar gyre circulation during the warm early- and mid-Holocene

Along with the enhanced influence of subtropical waters at mid-latitudes, published geochemical evidence also suggests a gradual increase in convection within the subpolar gyre during the early Holocene. Starting ~11 ka, paired Mg/Ca- $\delta^{18}$ O measurements of the thermocline species *G. inflata* (Figure 2b) suggest that subsurface waters just south of Iceland became fresher and colder over time (Thornalley et al., 2009). Since subsurface water in the inter-gyre reflect the mixing of two end-members, subpolar and subtropical mode waters, this subsurface freshening and cooling in the subsurface, in contrast to the warmer surface SST-alk, is consistent with the interpretation of enhanced ventilation and increased mode water formation in the subpolar gyre (Thornalley et al., 2009).

Primary productivity indices, based on our total concentration of alkenones, C37<sub>total</sub>, also support increased ventilation in the subpolar region during ~11-6 ka (Figure 2c). In the present day, the maintenance and variability of nutrient supply to the central and western North Atlantic are sensitive to subpolar gyre circulation. Increased wind stress enhances nutrient supply to the euphotic zone through stronger convective mixing and horizontal Ekman transport (Hátún et al., 2017; Williams & Follows, 1998; Williams et al., 2000). At ODP U1304, C37<sub>total</sub> covaries inversely with subsurface salinity and temperature



235

240

245

250

255

260



anomalies just south of Iceland (Figure 2b and c), suggesting higher primary productivity during periods of intensified subpolar gyre ventilation.

Another piece of evidence for a better ventilated subpolar gyre during the mid-Holocene comes from  $\varepsilon$ Nd isotopes derived from deep-sea corals in the northern Rockall Trough (747 meters, Colin et al., 2010). In the North Atlantic, seawater  $\varepsilon$ Nd can be interpreted as a mixture of two isotopic end-members: the more radiogenic subtropical water ( $\varepsilon$ Nd = -10 to -11) and the less radiogenic Subpolar Mode Water ( $\varepsilon$ Nd = -15 to -14) (Colin et al., 2010; Lacan and Jeandel, 2004). The significantly depleted  $\varepsilon$ Nd values observed during the mid-Holocene (Figure 2c) thus agree with a strong subpolar gyre circulation, which would have supplied a large volume of relatively fresh and cold subpolar mode water eastward into the subsurface of the inter-gyre region, as indicated by the Mg/Ca- $\delta$ <sup>18</sup>O data.

The influence of the subpolar gyre appears to have peaked between ~6-8ka (Figure 2b, c). During this time period, the relative abundance of the "Gulf-Stream" subsurface species *G. inflata* declined at ODP U1304, while the subpolar species *G. bulloides* became more abundant (Figure 2d). This competition between subpolar and subtropical waters in the inter-gyre region is also seen in the modern ocean on decadal timescales (Häkkinen and Rhines, 2004; Hátún et al., 2005). In case of the mid-Holocene, the termination of deglaciation after ~8 ka likely promoted ventilation in the Labrador Sea, allowing the subpolar gyre to strengthen (Solignac et al., 2004; and also see Thornalley et al., 2009), resulting in increased influence of subpolar waters. Nevertheless, the effects of stronger subpolar convection appear to have been limited to subsurface layers or winter conditions. At ODP U1304, SST-alk remained warm between ~11-6 ka. Similarly, diatom and foraminifera assemblages from the Nordic Sea indicate optimal conditions persisting until ~ 7ka (Andersson et al., 2010; Koç et al., 1993).

#### 6.2.3 Weakened subpolar gyre in the late Holocene

A major change in the mode of inter-gyre circulation occurred at ~6 ka. Coincident with the rapid cooling in SST-alk at ODP U1304 (Figure 2d), the subpolar gyre appears to have weakened. Reduced alkenone productivity indicated by C37<sub>total</sub> at the studied site (Figure 2c) suggests a decline in the southward mixing of nutrient-rich subpolar water. Meanwhile, subsurface temperature and salinity south of Iceland increased (Figure 2b), a change interpreted as indicative of reduced intermediate water formation in the Labrador Sea and a weakening of subpolar gyre ventilation (Thornalley et al., 2009). A weakened subpolar gyre is further supported by £Nd isotope records (Figure 2c). The more radiogenic sub-surface water indicates that less subpolar mode water has been advected to the eastern basin in the late Holocene (Colin et al., 2010).

#### 6.2.4 Weakened subtropical circulation in the late Holocene



265



Unlike the early- to mid-Holocene (8~11ka), a weaker subpolar gyre over the last 6 kyrs does not appear to have been compensated by a recovery in subtropical circulation at mid-latitudes. At ODP U1304, the abundance of the Gulf Stream subsurface species *G. inflata* has remained low since ~8 ka (Figure 2d Yellow shading), while tropical species have been entirely absent (Pink shading). Similarly, diatom records from the Nordic Sea indicate that by 5 ka, warm Atlantic water masses had retreated, and Arctic species had expanded north of Iceland (Koç et al., 1993). Increased input of IRD in the last few millennials (Figure 2a) further suggests a reduced influence of Atlantic-sourced warm waters (Moros et al., 2006; Perner et al., 2016). Clearly, the influence of the NAC in mid- and high-latitude regions reduced during the late Holocene.

To investigate changes in the subtropical gyre during the late Holocene, we examined two additional indices from the subtropical North Atlantic: (1) upwelling intensity west of North Africa, and (2) the E-W SST gradient across the subtropic North Atlantic. Both indices can be used to qualitatively assess changes in wind-driven subtropical gyre circulation.

Specifically, the theory of mid-latitude stationary waves links the summer development of North Atlantic subtropical anticyclones to latent heat released over northern continents during the advance of summer monsoons (Hoskins, 1996; Mantsis et al., 2013). During the mid-Holocene, large diabatic heating anomalies associated with enhanced convective precipitation in northern continents should have favored the development of stronger subtropical anticyclones (Mantsis et al., 2013; Rodwell & Hoskins, 2001). Enhanced subsidence of dry air and stronger easterly trade winds associated with these anticyclones would promote upwelling and sea surface cooling in the northern tropical Atlantic (Red arrow in Figure 1a).

This cooling associated with tropical upwelling is well documented in the planktonic foraminiferal assemblages at ODP 658 (Figure 2e, from deMenocal et al., 2000), characterized by the dominance of *G. bulloides*—a species indicative of nutrient-rich upwelling waters at low latitudes.

Enhanced summer heating should have also promoted a stronger subtropical anticyclone with northward and westward expansion (Mantsis et al., 2013), favoring sea surface warming in the western subtropical Atlantic (Seager et al., 2003). Consistent with this, SST-alk records indicate relatively warm conditions in the western basin (Sachs, 2007). More importantly, the warming in the west and cooling in the east during this period gave rise to a positive SST gradient between GGC 19 (37°N) and ODP 658 (21°N) (Figure 4a solid line).

In the late Holocene, reduced summer insolation led to a weakening of subtropical anticyclone. This weakening, combined with an equatorward shift in the mean position of the inter-gyre circulation and the NAC, particularly during summer, accounts for the rapid cooling observed at ODP U1304 ~6 ka, as well as the pronounced cooling recorded at GGC 19, 26, and 30. In the eastern subtropical basin, weakened easterlies, associated with the decline in African Monsoon after 5 ka,



300

310

315

320



resulted in reduced upwelling intensity (deMenocal et al., 2000). Consequently, the east-west SST gradient reversed (Figure 4a).

#### 7 Model-data discrepancy

The discussions above provide empirical evidence of dynamic inter-gyre circulation during the Holocene. In this section, we compare our results with the TraCE-21K simulation. TraCE-21K is a transient global climate model that uses the fully coupled CCSM3 to simulate climatic evolution since 21 ka (He, 2011). Because it successfully reproduces many major features of postglacial climate dynamics, including abrupt climate changes, TraCE-21K has been widely used in studies of climate evolution since the Last Glacial Maximum (Erb et al., 2022; Liu et al., 2009, 2014; Marcott et al., 2011).

We first calculated the annual mean ΔSST between 6–8 ka and 0–2 ka in the TraCE-21K simulation. As shown in Figure 1b, the model simulates basin-wide warming over the past 6 kyr (color shading), which is not reflected in the ΔSST-alk data (blue numbers), either in terms of the sign of change or spatial pattern. We also calculated two SST gradients in the TraCE-21K model: (1) ΔSST between ODP U1304 and U1308 in the subpolar, and (2) ΔSST between GGC26 and ODP 658 across the subtropical North Atlantic (Figure 4). Again, the model shows no significant change in these gradients (dashed lines), in contrast to the proxy records.

Considering that SST-alk is likely seasonally biased, we also examined changes in summer temperatures (June, July, August) between 6–8 ka and 0–2 ka in the TraCE-21K simulation (Figure S3a). Although some cooling is observed along the coast of Greenland, the model still shows basin-wide warming in the mid-latitudes. This suggests that the data–model discrepancy cannot be simply attributed to an artifact of comparing seasonally biased proxies with modeled annual mean temperatures.

We additionally analyzed SST results from the TraCE-21K-II simulations. TraCE-21K-II is a modified version of TraCE-21K with the same climatic forcing, but without freshwater fluxes into the North Atlantic throughout the Holocene, designed to better align the modeled AMOC temporal variability with proxy reconstructions. (<sup>231</sup>Pa/<sup>230</sup>Th ratio from Bermuda Rise) (He and Clark, 2022b). We calculated both summer and annual mean ΔSST between 6–8 ka and 0–2 ka in TraCE-21K-II (Figure S3b, c). The annual mean ΔSST again shows basin-wide warming. Changes in summer temperatures, on the other hand, show some improvement, with no warming in the subpolar gyre during the late Holocene. Nevertheless, the zonally asymmetric cooling is still not well represented.

In Section 6, we linked  $\Delta$ SST-alk changes to variations in inter-gyre circulation using proxy records. It is therefore reasonable to speculate that the models' misrepresentation of the  $\Delta$ SST pattern may also reflect an inadequate representation



340

345



of inter-gyre circulation dynamics. To illustrate this point, we perform two additional analyses: first, we calculate the horizontal SST gradient, and second, we examine the Holocene wind stress curl pattern in TraCE-21K.

The most interesting feature is that the maximum horizontal SST gradient and the corresponding zero wind-stress-curl line in the model are located at ~40°N, maintaining a nearly W-E zonal orientation (Figure 5 and 3b). This stands in sharp contrast to modern observations, which exhibit a distinct SE-NE tilt. Furthermore, the wind-stress curl distribution during the 6–8 ka period shows little difference from that of the last 2 kyr in the model (Figure S5), suggesting that the inter-gyre circulation remains largely invariant throughout the Holocene in the simulation. A comparable, temporally stable SST gradient is also evident in the TraCE-21K-II model (Figure S4).

Overall, our analyses indicate that the inter-gyre circulation and the NAC in the model do not behave as they do in the modern ocean, nor as they are inferred to have operated during the mid-Holocene. What might explain this model misrepresentation? While a comprehensive discussion of this issue is beyond the scope of this study, and may also be model-dependent, we propose two tentative explanations.

An immediate reason may lie in the model's limitation to capture the substantial cooling of the subpolar gyre during the late Holocene. Paleoclimate evidence indicates that the late Holocene was marked by increased Arctic freshwater export into the subpolar gyre via the East Greenland Current (EGC) and intensified atmospheric westerlies, both of which contributed to cooling and freshening across the central subpolar gyre and reduced influence of Atlantic waters in the Denmark Strait after ~4-5 ka (Morley et al., 2014; Moros et al., 2012). While the model does simulate some degree of coastal cooling along Greenland (Figure S3, S4), it does not reproduce the widespread cooling observed across the subpolar and inter-gyre regions. The associated southward shift of the Subarctic Front (SAF) is also not adequately represented in simulations.

On the other hand, our analysis also indicate that model appear unable to simulate inter-gyre circulation with its SE-NE tilt during both the middle and late Holocene, let along its time variations. It has recently been recognized that model resolution is crucial for accurately representing midlatitude western boundary currents and their associated eddies (Chassignet and Marshall, 2008; Chassignet and Xu, 2017; Hirschi et al., 2020; Maltrud and McClean, 2005). The coarse horizontal resolution characteristic of long transient simulations, such as TraCE-21k, may partially explain why the mean geometry of inter-gyre circulation and temporal variability are not well resolved.

# **8 Conclusions**

Holocene global temperature estimates yield conflicting results between proxy reconstructions and model simulations, raising questions about the relative importance of CO<sub>2</sub> and orbital forcing in determining global climate sensitivity, as well

https://doi.org/10.5194/egusphere-2025-5181 Preprint. Discussion started: 29 October 2025

© Author(s) 2025. CC BY 4.0 License.





360 as about the robustness of paleoclimate reconstructions. In this study, we use alkenone-derived sea surface temperatures

(SSTs) to examine the spatial and temporal trends of SST changes in the inter-gyre North Atlantic. We also integrate

planktonic foraminifera assemblages with published geochemical records to investigate circulation changes within these

mid-latitude frontal systems associated with cooling. We find that:

365 (1) The late-Holocene summertime cooling in the North Atlantic is characterized by an increased zonal SST gradient in the

mid-latitude inter-gyre region, with greater cooling in the west than in the east. This zonal asymmetry suggests that the

cooling cannot be attributed to a direct response to local summer insolation changes.

(2) Multiple lines of evidence suggest that the spatial pattern of  $\Delta$ SST-alk is associated with changes in inter-gyre

circulation. The poor representation of the position and orientation of the inter-gyre circulation in the mid-latitude North

Atlantic in models accounts for the observed data-model discrepancies.

#### **Competing interests**

370

375

The authors declare no competing interests

# Code and data availability

Data generated in this study is available as online supplementary materials.

# Acknowledgments

380 This work is partially supported by NSF-OCE 2202760 and 2410906 to W. Si and T. Herbert.





Figure 1. (a) Sites examined in this study. Black stars: Alkenone-derived SST (SST-alk); see Table S1 for a complete reference list. Open star: Paired Mg/Ca –δ<sup>18</sup>O analysis of planktonic foraminifera (Thornalley et al., 2009). Orange square: Coral εNd (Colin et al., 2010). Pink stars: Ice Rafted debris. Color shading: modern annual mean SST (OISST). (b) model-data comparison of ΔSST between two time slices (0-2 ka minus 6-8 ka). Blue numbers: ΔSST-alk. Color shading: ΔSST from the TraCE-21K model.

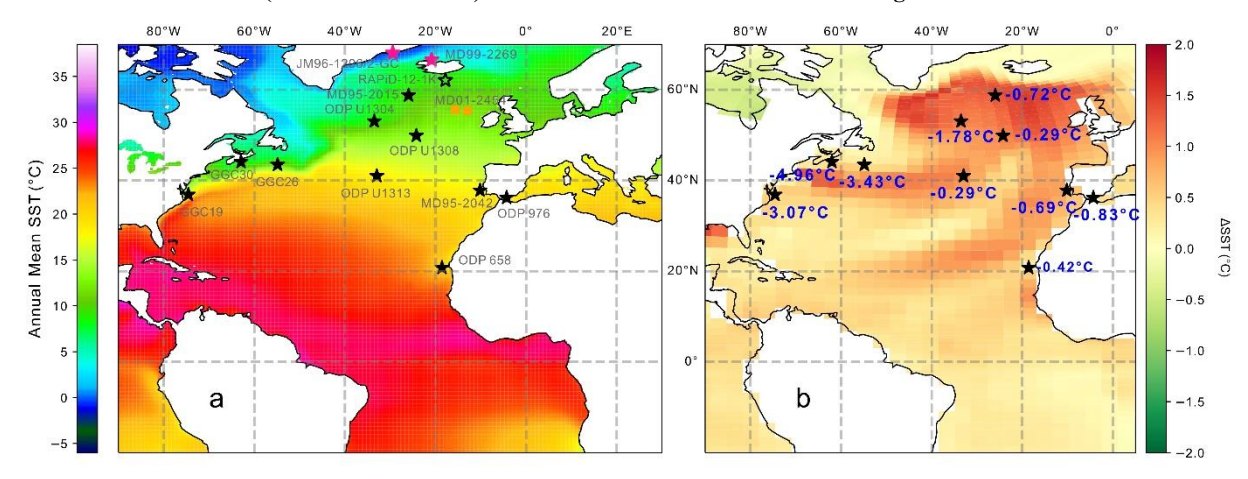
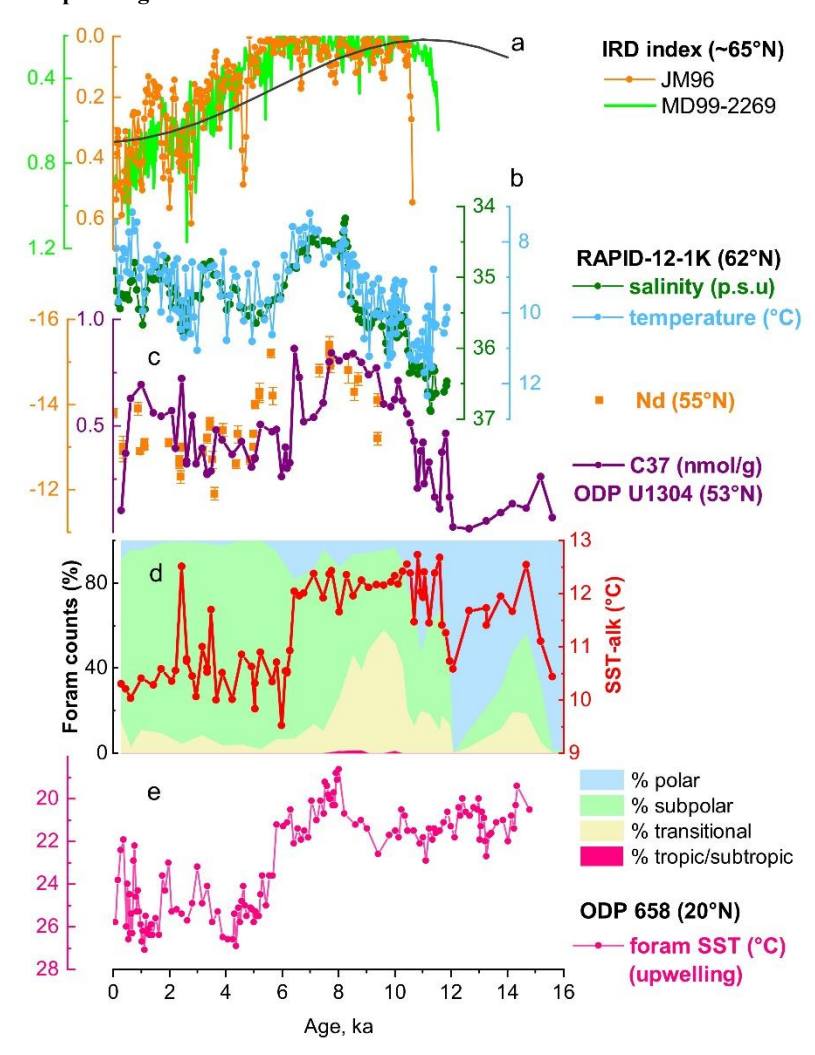






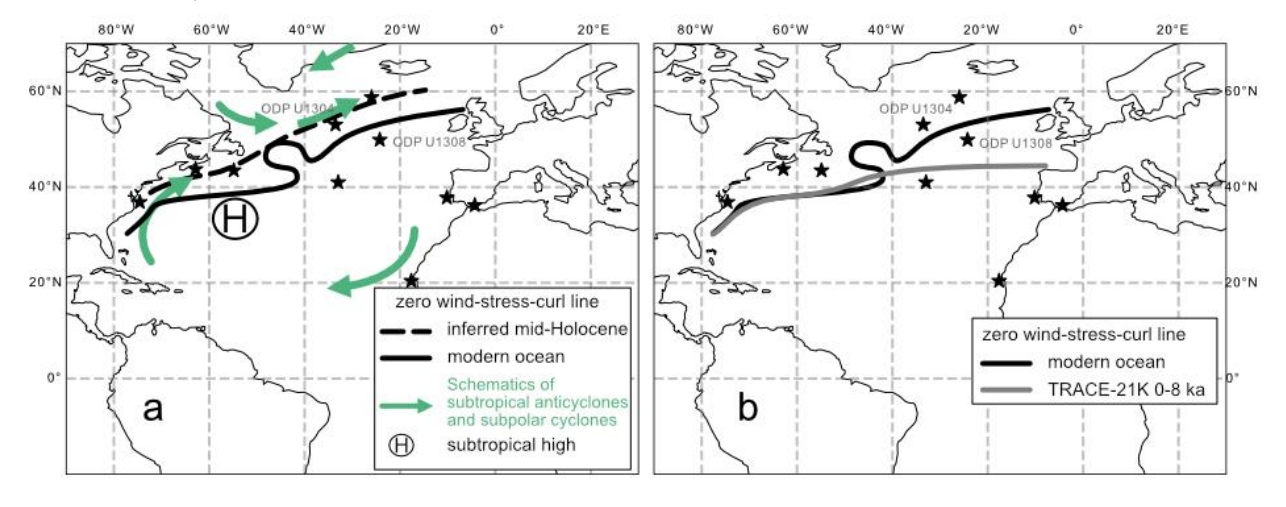
Figure 2. Late Holocene paleo-proxies from the North Atlantic. (a) Black curve, June 21st insolation at 65°N; Orange circles, IRD counts from the Eastern Greenland shelf site (JM96-1206/2-GC) (Perner et al., 2016); Green line: Proportion of "foreign" IRD, interpreted as a proxy for sea-ice drift (Moros et al., 2006). (b) Subsurface temperature and salinity estimates from paired Mg/Cavanalyses of *G. inflata* (Thornalley et al., 2009). (c) Purple: C37<sub>total</sub> of ODP U1304, Orange: coral ENd (Colin et al., 2010). (d) Red line: SST-alk of ODP U1304, Color shading: relative abundance of planktonic foraminifera from ODP U1304. (e): Pink line: SST from ODP Site 658, estimated from foraminiferal assemblage analysis (Demenocal et al., 2000), which may also be interpreted as an upwelling index







400 Figure 3. Comparison of (a) reconstructed and (b) modeled mid-Holocene inter-gyre circulation. (a): During the early and mid-Holocene, proxy evidence suggests that the inter-gyre circulation was likely strengthened and shifted northward relative to its present position. (b): In contrast, in the TraCE-21K simulation, the annual mean zero wind-stress curl line remained nearly zonal over the last 8 kyrs.

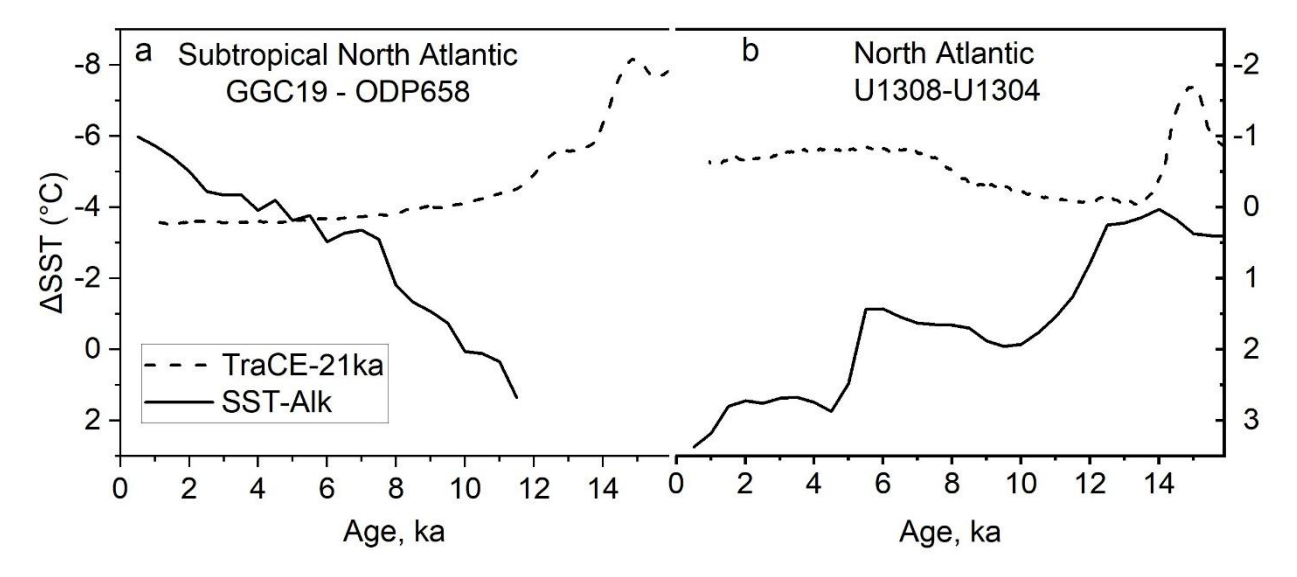


405





Figure 4. Changes in SST gradients across (a) the subtropical North Atlantic and (b) the mid-latitude North Atlantic.

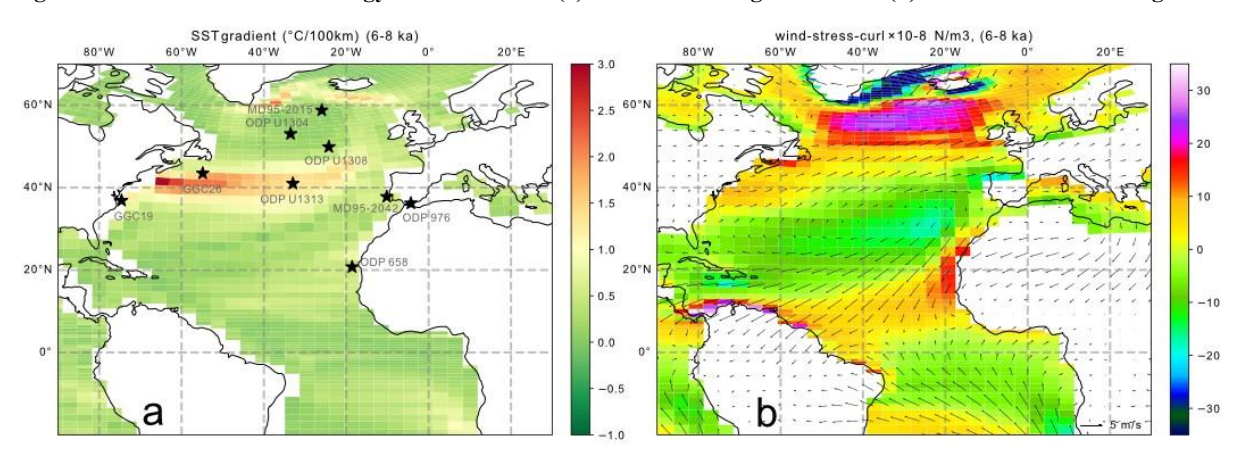


410





# Figure 5: North Atlantic climatology in TraCE-21K: (a) horizontal SST gradient and (b) wind-stress-curl during 6-8 ka.







#### References

- 420 Andersson, C., Pausata, F. S., Jansen, E., Risebrobakken, B., and Telford, R. J.: Holocene trends in the foraminifer record from the Norwegian Sea and the North Atlantic Ocean, Climate of the Past, 6, 179–193, 2010.
  - Bova, S., Rosenthal, Y., Liu, Z., Godad, S. P., and Yan, M.: Seasonal origin of the thermal maxima at the Holocene and the last interglacial, nature, 589, 548–553, 2021.
- Came, R. E., Oppo, D. W., and McManus, J. F.: Amplitude and timing of temperature and salinity variability in the subpolar North Atlantic over the past 10 ky, Geology, 35, 315–318, 2007.
  - Chassignet, E. P. and Marshall, D. P.: Gulf Stream separation in numerical ocean models, Geophysical Monograph Series, 177, 2008.
  - Chassignet, E. P. and Xu, X.: Impact of horizontal resolution (1/12 to 1/50) on Gulf Stream separation, penetration, and variability, Journal of Physical Oceanography, 47, 1999–2021, 2017.
- Colin, C., Frank, N., Copard, K., and Douville, E.: Neodymium isotopic composition of deep-sea corals from the NE Atlantic: implications for past hydrological changes during the Holocene, Quaternary Science Reviews, 29, 2509–2517, 2010.
  - Czaja, A. and Marshall, J.: Observations of atmosphere-ocean coupling in the North Atlantic, Quarterly Journal of the Royal Meteorological Society, 127, 1893–1916, 2001.
- Demenocal, P., Ortiz, J., Guilderson, T., Adkins, J., Sarnthein, M., Baker, L., and Yarusinsky, M.: Abrupt onset and termination of the African Humid Period:: rapid climate responses to gradual insolation forcing, Quaternary science reviews, 19, 347–361, 2000.
- Emile-Geay, J., Cane, M. A., Naik, N., Seager, R., Clement, A. C., and van Geen, A.: Warren revisited: Atmospheric freshwater fluxes and "Why is no deep water formed in the North Pacific," Journal of Geophysical Research: Oceans, 108, 2003.
  - Erb, M. P., McKay, N. P., Steiger, N., Dee, S., Hancock, C., Ivanovic, R. F., Gregoire, L. J., and Valdes, P.: Reconstructing Holocene temperatures in time and space using paleoclimate data assimilation, EGUsphere, 1–48, 2022.
  - Häkkinen, S. and Rhines, P. B.: Decline of subpolar North Atlantic circulation during the 1990s, Science, 304, 555-559, 2004.
- Häkkinen, S., Rhines, P. B., and Worthen, D. L.: Warm and saline events embedded in the meridional circulation of the northern North Atlantic, Journal of Geophysical Research: Oceans, 116, 2011.
  - Häkkinen, S., Rhines, P. B., and Worthen, D. L.: Northern North Atlantic sea surface height and ocean heat content variability, Journal of Geophysical Research: Oceans, 118, 3670–3678, 2013.
- Hátún, H., Sandø, A. B., Drange, H., Hansen, B., and Valdimarsson, H.: Influence of the Atlantic subpolar gyre on the thermohaline circulation, Science, 309, 1841–1844, 2005.
  - Hátún, H., Azetsu-Scott, K., Somavilla, R., Rey, F., Johnson, C., Mathis, M., Mikolajewicz, U., Coupel, P., Tremblay, J.-É., and Hartman, S.: The subpolar gyre regulates silicate concentrations in the North Atlantic, Scientific reports, 7, 1–9, 2017.





- He, F.: Simulating transient climate evolution of the last deglaciation with CCSM 3, 2011.
- He, F. and Clark, P. U.: Freshwater forcing of the atlantic meridional overturning circulation revisited, Nature Climate Change, 12, 449–454, 2022a.
  - He, F. and Clark, P. U.: Freshwater forcing of the atlantic meridional overturning circulation revisited, Nature Climate Change, 12, 449–454, 2022b.
- Hirschi, J. J., Barnier, B., Böning, C., Biastoch, A., Blaker, A. T., Coward, A., Danilov, S., Drijfhout, S., Getzlaff, K., and Griffies, S. M.: The Atlantic meridional overturning circulation in high-resolution models, Journal of Geophysical Research:
  Oceans, 125, e2019JC015522, 2020.
  - Hodell, D. A., Evans, H. F., Channell, J. E., and Curtis, J. H.: Phase relationships of North Atlantic ice-rafted debris and surface-deep climate proxies during the last glacial period, Quaternary Science Reviews, 29, 3875–3886, 2010.
  - Hoskins, B.: On the existence and strength of the summer subtropical anticyclones: Bernhard Haurwitz memorial lecture, Bulletin of the American Meteorological Society, 77, 1287–1292, 1996.
- Huang, B., Liu, C., Banzon, V., Freeman, E., Graham, G., Hankins, B., Smith, T., and Zhang, H.-M.: Improvements of the daily optimum interpolation sea surface temperature (DOISST) version 2.1, Journal of Climate, 34, 2923–2939, 2021.
  - Jonkers, L. and Kučera, M.: Sensitivity to species selection indicates the effect of nuisance variables on marine microfossil transfer functions, Climate of the Past, 15, 881–891, 2019.
- Kaufman, D., McKay, N., Routson, C., Erb, M., Dätwyler, C., Sommer, P. S., Heiri, O., and Davis, B.: Holocene global mean surface temperature, a multi-method reconstruction approach, Scientific data, 7, 1–13, 2020.
  - Kelly, P., Kravitz, B., Lu, J., and Leung, L. R.: Remote drying in the North Atlantic as a common response to precessional changes and CO2 increase over land, Geophysical Research Letters, 45, 3615–3624, 2018.
- Kim, J.-H., Rimbu, N., Lorenz, S. J., Lohmann, G., Nam, S.-I., Schouten, S., Rühlemann, C., and Schneider, R. R.: North Pacific and North Atlantic sea-surface temperature variability during the Holocene, Quaternary Science Reviews, 23, 2141–2154, 2004.
  - Koç, N., Jansen, E., and Haflidason, H.: Paleoceanographic reconstructions of surface ocean conditions in the Greenland, Iceland and Norwegian seas through the last 14 ka based on diatoms, Quaternary Science Reviews, 12, 115–140, 1993.
  - Lacan, F. and Jeandel, C.: Subpolar Mode Water formation traced by neodymium isotopic composition, Geophysical Research Letters, 31, 2004.
- 480 Lawrence, K. T., Liu, Z., and Herbert, T. D. %J S.: Evolution of the eastern tropical Pacific through Plio-Pleistocene glaciation, 312, 79–83, 2006.
  - Leduc, G., Schneider, R., Kim, J.-H., and Lohmann, G.: Holocene and Eemian sea surface temperature trends as revealed by alkenone and Mg/Ca paleothermometry, Quaternary Science Reviews, 29, 989–1004, 2010.
- Linsley, B. K., Rosenthal, Y., and Oppo, D. W.: Holocene evolution of the Indonesian throughflow and the western Pacific warm pool, Nature Geoscience, 3, 578–583, 2010.





- Liu, Y., Zhang, M., Liu, Z., Xia, Y., Huang, Y., Peng, Y., and Zhu, J.: A possible role of dust in resolving the Holocene temperature conundrum, scientific Reports, 8, 1–9, 2018.
- Liu, Z., Otto-Bliesner, B., He, F., Brady, E., Tomas, R., Clark, P., Carlson, A., Lynch-Stieglitz, J., Curry, W., and Brook, E.: Transient simulation of last deglaciation with a new mechanism for Bølling-Allerød warming, Science, 325, 310–314, 2009.
- 490 Liu, Z., Zhu, J., Rosenthal, Y., Zhang, X., Otto-Bliesner, B. L., Timmermann, A., Smith, R. S., Lohmann, G., Zheng, W., and Timm, O. E.: The Holocene temperature conundrum, Proceedings of the National Academy of Sciences, 111, E3501–E3505, 2014.
- Losa, S. N., Soppa, M. A., Dinter, T., Wolanin, A., Brewin, R. J., Bricaud, A., Oelker, J., Peeken, I., Gentili, B., and Rozanov, V.: Synergistic exploitation of hyper-and multi-spectral precursor sentinel measurements to determine phytoplankton functional types (SynSenPFT), Frontiers in Marine Science, 4, 203, 2017.
  - Lougheed, B. C. and Obrochta, S.: A Rapid, Deterministic age-depth modeling routine for geological sequences with inherent depth uncertainty, Paleoceanography and Paleoclimatology, 34, 122–133, 2019.
  - Maltrud, M. E. and McClean, J. L.: An eddy resolving global 1/10 ocean simulation, Ocean Modelling, 8, 31–54, 2005.
- Mantsis, D. F., Clement, A. C., Kirtman, B., Broccoli, A. J., and Erb, M. P.: Precessional cycles and their influence on the North Pacific and North Atlantic summer anticyclones, Journal of climate, 26, 4596–4611, 2013.
  - Marchal, O., Cacho, I., Stocker, T. F., Grimalt, J. O., Calvo, E., Martrat, B., Shackleton, N., Vautravers, M., Cortijo, E., and van Kreveld, S.: Apparent long-term cooling of the sea surface in the northeast Atlantic and Mediterranean during the Holocene, Quaternary Science Reviews, 21, 455–483, 2002.
- Marcott, S. A., Clark, P. U., Padman, L., Klinkhammer, G. P., Springer, S. R., Liu, Z., Otto-Bliesner, B. L., Carlson, A. E., Ungerer, A., and Padman, J.: Ice-shelf collapse from subsurface warming as a trigger for Heinrich events, Proceedings of the National Academy of Sciences, 108, 13415–13419, 2011.
  - Marcott, S. A., Shakun, J. D., Clark, P. U., and Mix, A. C.: A reconstruction of regional and global temperature for the past 11,300 years, science, 339, 1198–1201, 2013.
- Marshall, J., Johnson, H., and Goodman, J.: A study of the interaction of the North Atlantic Oscillation with ocean circulation, Journal of Climate, 14, 1399–1421, 2001.
  - Marzocchi, A., Hirschi, J. J.-M., Holliday, N. P., Cunningham, S. A., Blaker, A. T., and Coward, A. C.: The North Atlantic subpolar circulation in an eddy-resolving global ocean model, Journal of Marine Systems, 142, 126–143, 2015.
  - McCarthy, G. D., Haigh, I. D., Hirschi, J. J.-M., Grist, J. P., and Smeed, D. A.: Ocean impact on decadal Atlantic climate variability revealed by sea-level observations, Nature, 521, 508–510, 2015.
- Morley, A., Rosenthal, Y., and DeMenocal, P.: Ocean-atmosphere climate shift during the mid-to-late Holocene transition, Earth and Planetary Science Letters, 388, 18–26, 2014.
  - Moros, M., Andrews, J. T., Eberl, D. D., and Jansen, E.: Holocene history of drift ice in the northern North Atlantic: Evidence for different spatial and temporal modes, Paleoceanography, 21, 2006.
- Moros, M., Jansen, E., Oppo, D. W., Giraudeau, J., and Kuijpers, A.: Reconstruction of the late-Holocene changes in the Sub-Arctic Front position at the Reykjanes Ridge, north Atlantic, The Holocene, 22, 877–886, 2012.





- Müller, P. J., Kirst, G., Ruhland, G., Von Storch, I., and Rosell-Melé, A.: Calibration of the alkenone paleotemperature index U37K' based on core-tops from the eastern South Atlantic and the global ocean (60 N-60 S), Geochimica et Cosmochimica Acta, 62, 1757–1772, 1998.
- Osman, M. B., Tierney, J. E., Zhu, J., Tardif, R., Hakim, G. J., King, J., and Poulsen, C. J.: Globally resolved surface temperatures since the Last Glacial Maximum, 2021.
  - Park, H.-S., Kim, S.-J., Stewart, A. L., Son, S.-W., and Seo, K.-H.: Mid-Holocene Northern Hemisphere warming driven by Arctic amplification, Science advances, 5, eaax8203, 2019.
- Perner, K., Jennings, A. E., Moros, M., Andrews, J. T., and Wacker, L.: Interaction between warm Atlantic-sourced waters and the East Greenland Current in northern Denmark Strait (68 N) during the last 10 600 cal a BP, Journal of Quaternary Science, 31, 472–483, 2016.
  - Raja, M. and Rosell-Melé, A.: Appraisal of sedimentary alkenones for the quantitative reconstruction of phytoplankton biomass, Proceedings of the National Academy of Sciences, 118, 2021.
  - Rodwell, M. J. and Hoskins, B. J.: Subtropical anticyclones and summer monsoons, Journal of Climate, 14, 3192-3211, 2001.
- Rossby, T.: The North Atlantic Current and surrounding waters: At the crossroads, Reviews of Geophysics, 34, 463–481, 1996.
  - Ruddiman, W. F.: Historical stability of the Gulf Stream meander belt: foraminiferal evidence, Deep Sea Research and Oceanographic Abstracts, 137–148, 1968.
- Ruddiman, W. F. and Esmay, A.: A Streamlined Foraminiferal Transfer-function for the Subpolar North-Atlantic, Initial Reports of the Deep Sea Drilling Project, 94, 1045–1057, 1987.
  - Sachs, J. P.: Cooling of Northwest Atlantic slope waters during the Holocene, Geophysical research letters, 34, 2007.
  - Salvigsen, O., Forman, S. L., and Miller, G. H.: Thermophilous molluscs on Svalbard during the Holocene and their paleoclimatic implications, Polar Research, 11, 1–10, 1992.
- Seager, R., Murtugudde, R., Naik, N., Clement, A., Gordon, N., and Miller, J.: Air–sea interaction and the seasonal cycle of the subtropical anticyclones, Journal of climate, 16, 1948–1966, 2003.
  - Shuman, B. N. and Marsicek, J.: The structure of Holocene climate change in mid-latitude North America, Quaternary Science Reviews, 141, 38–51, 2016.
  - Siegel, D., Doney, S., and Yoder, J.: The North Atlantic spring phytoplankton bloom and Sverdrup's critical depth hypothesis, science, 296, 730–733, 2002.
- Solignac, S., de Vernal, A., and Hillaire-Marcel, C.: Holocene sea-surface conditions in the North Atlantic—contrasted trends and regimes in the western and eastern sectors (Labrador Sea vs. Iceland Basin), Quaternary Science Reviews, 23, 319–334, 2004.
  - Thompson, A. J., Zhu, J., Poulsen, C. J., Tierney, J. E., and Skinner, C. B.: Northern Hemisphere vegetation change drives a Holocene thermal maximum, Science advances, 8, eabj6535, 2022.





- Thornalley, D. J., Elderfield, H., and McCave, I. N.: Holocene oscillations in temperature and salinity of the surface subpolar North Atlantic, Nature, 457, 711–714, 2009.
  - Thornalley, D. J., McCave, I. N., and Elderfield, H.: Tephra in deglacial ocean sediments south of Iceland: Stratigraphy, geochemistry and oceanic reservoir ages, Journal of Quaternary Science, 26, 190–198, 2011.
- Tierney, J. E. and Tingley, M. P.: BAYSPLINE: A new calibration for the alkenone paleothermometer, Paleoceanography and Paleoclimatology, 33, 281–301, 2018.
  - Toggweiler, J. and Si, W.: A new role for the AMOC during the ice ages, Paleoceanography and Paleoclimatology, 40, e2024PA004973, 2025.
  - Volkov, D. L., Baringer, M., Smeed, D., Johns, W., and Landerer, F. W.: Teleconnection between the Atlantic meridional overturning circulation and sea level in the Mediterranean Sea, Journal of climate, 32, 935–955, 2019.
- 565 Warren, B. A.: Why is no deep water formed in the North Pacific?, Journal of Marine Research, 41, 327–347, 1983.
  - Werner, K., Spielhagen, R. F., Bauch, D., Hass, H. C., and Kandiano, E.: Atlantic Water advection versus sea-ice advances in the eastern Fram Strait during the last 9 ka: Multiproxy evidence for a two-phase Holocene, Paleoceanography, 28, 283–295, 2013.
- Williams, R. G., McLaren, A. J., and Follows, M. J.: Estimating the convective supply of nitrate and implied variability in export production over the North Atlantic, Global Biogeochemical Cycles, 14, 1299–1313, 2000.
  - Yang, H., Lohmann, G., Krebs-Kanzow, U., Ionita, M., Shi, X., Sidorenko, D., Gong, X., Chen, X., and Gowan, E. J.: Poleward shift of the major ocean gyres detected in a warming climate, Geophysical Research Letters, 47, e2019GL085868, 2020.
- Zhao, M., Beveridge, N., Shackleton, N., Sarnthein, M., and Eglinton, G.: Molecular stratigraphy of cores off northwest Africa: Sea surface temperature history over the last 80 ka, Paleoceanography, 10, 661–675, 1995.